Available online at www.sciencedirect.com

ScienceDirect

ARTICLE

Effects and Optimization of Roll Sizes in Hot Rolling of Large Rings of Titanium Alloy

Wang Min,   Yang He,   Guo Lianggang,   Sun Zhichao

Northwestern Polytechnical University, Xi'an 710072, China

Abstract: In hot rolling of large rings of titanium alloy (LRTs), the ratio of roll radii R_1/R_2, i.e., the ratio of the radius of the driver roll R_1 to that of the idle roll R_2, has a significant effect on the geometric shape of the deformation zone (GSDZ) which plays a decisive role in achieving LRTs with high quality. In the study, an analytical description of the GSDZ is presented, and quantitative relationships between the GSDZ and R_1/R_2 are determined. Then a validated coupled thermo-mechanical 3D-FE model of the process is developed in the dynamic explicit code ABAQUS/Explicit. Finally, an investigation is conducted regarding the effects of R_1/R_2 on the quality of LRTs from the view point of GSDZ using FE simulation. The results show that there is an optimized range of R_1/R_2 for obtaining LRTs with better end-plane quality and more uniform strain and temperature distributions.

Key words: large ring of titanium alloy; hot ring rolling; roll size; dynamic explicit FEM; coupled thermal-mechanical effect

The large rings of titanium alloy (LRTs) with outer diameters greater than 1 m have been found wide applications in industry fields. Hot ring rolling is an advanced forming technology and a main processing method for producing LRTs due to its advantages such as considerable saving in energy and material costs, high quality and high efficiency.

In hot rolling of a LRT, the quality of the ring strongly relies on the geometric shape of the deformation zone (GSDZ) because the latter controls the mechanical and thermal behaviours of the ring. Of all the factors governing the GSDZ, the ratio of rolls' radii R_1/R_2, i.e., the ratio of the radius of the driver roll R_1 to that of the idle roll R_2, is a crucial one. Therefore, optimized values of R_1/R_2 are helpful to obtaining LRTs with high quality. However, an insight into the effects of R_1/R_2 should be gained first in order to achieve the optimized R_1/R_2. Xu et al.[1] adopted the upper bound method to make a preliminary analysis of the effects of R_1/R_2 on force and power parameters, etc., but they did not clarify the mechanism of the effects. Other literatures available concerning with the effects of R_1/R_2 on ring rolling are scant.

Actually, hot rolling of LRTs is a large-scale and highly nonlinear problem with coupled thermal-mechanical effect, so it is quite difficult and cost-consuming to accurately analyze the process with analytical and/or experimental methods. Since the dynamic explicit FEM can efficiently deal with large-scale and highly nonlinear problems, it was applied for hot ring rolling by Xie et al.[2] and Wang et al.[3], but they did not consider the coupled effect of mechanical and thermal behaviors.

In the study, an analytical description of the GSDZ is presented, followed by the establishment of a validated coupled thermal-mechanical 3D-FE model for hot rolling of LRTs. An investigation is finally conducted regarding the effects of R_1/R_2 on the ring quality using FE simulation, and thus optimized values of R_1/R_2 are achieved. The achievements can serve as a guide to the design and optimization of roll sizes for the practice of relevant processes.

1 Analytical Description of the GSDZ

Fig.1 illustrates the 2D schematic diagram of hot ring rolling of a large ring, where the shadow region is just the deformation zone of the ring. In terms of deformation characteristics
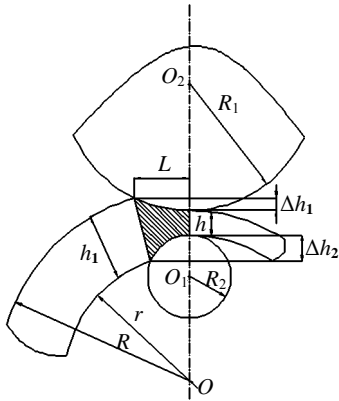
Fig.1   2D schematic diagram of hot ring rolling of a large ring

of hot ring rolling, two parameters are put forward to describe the GSDZ.

1.1   Average shape parameter $\bar{G}$

The shape parameter G is defined as

$$G=(L/h_a)^2 \tag{1}$$

where L and h_a are the length and average thickness of the deformation zone, respectively.

$$h_a=(h_1+h)/2=h+\Delta h/2 \approx h \tag{2}$$

where h_1 and h are the thicknesses at the entrance and at the exit of the deformation zone, respectively; Δh is feed amount per revolution of the ring.

L can be described by[4]

$$L=\sqrt{\frac{2\Delta h}{\frac{1}{R_1}+\frac{1}{R_2}+\frac{1}{R}-\frac{1}{r}}} \tag{3}$$

where R_1 and R_2 are the radius of the driver roll and idle roll, respectively; R and r are the outer and inner radius of the deformation ring, respectively.

For hot rolling of large ring, $\dfrac{1}{R}-\dfrac{1}{r}$ is such a small value

compared to $\dfrac{1}{R_1}+\dfrac{1}{R_2}$ that it can be neglected and, as a result,

Eq. (3) can be expressed by

$$L \approx \sqrt{\frac{2\Delta h}{\frac{1}{R_1}+\frac{1}{R_2}}} \tag{4}$$

Assuming no spread and no relative sliding between the ring and the driver roll, we have[5]

$$\Delta h = \frac{\pi v}{2n_1 R_1}\left(\frac{(R_0+r_0)h_0}{h}+h\right) \tag{5}$$

where v is the feed rate of the roll; n_1 is the rotational speed of the driver roll; h_0 is the initial thickness of the ring; R_0 and r_0 are the initial outer and inner radius of the ring, respectively.

Substituting Eqs. (2) , (4) and (5) into Eq. (1) gives

$$G = \frac{\pi v}{n_1}\cdot\frac{1}{1+R_1/R_2}\cdot\left(\frac{(R_0+r_0)h_0}{h^3}+\frac{1}{h}\right) \tag{6}$$

For a given rolling process，G is an instantaneous variable, changing monotonously with time, so its average value over the total rolling time T can be used for mathematical convenience, namely

$$\bar{G} = \int_0^T \left(\frac{\pi \bar{v}}{n_1}\cdot\frac{1}{1+R_1/R_2}\cdot\left(\frac{(R_0+r_0)h_0}{h^3}+\frac{1}{h}\right)\right)\mathrm{d}t/T \tag{7}$$

$$\bar{v} = \int_0^T v\,\mathrm{d}t/T \tag{8}$$

$$h = h_0 - \bar{v}t \tag{9}$$

where $\bar{v}$ is the average feed rate over T，and t is the time variable.

$\bar{G}$ describes the distribution state of plastic deformation along the radial thickness of the ring. Under the stable forming condition, with greater $\bar{G}$, plastic deformation tends to extend from the inside and outside layers to the middle layer of the ring, thus causing the strain distribution to become more uniform. Meanwhile, the restraint role of the middle layer on the inside and outside layers weakens and it is advantageous for the metal in the inside and outside layers to flow to the tangential direction of the ring, which makes the spread distribution become more uniform.

1.2   Average distribution ratio of feed amount $\bar{\gamma}$

Actually, Δh is composed of Δh_1, feed amount per revolution at the outside of the ring and Δh_2, at the inside of the ring. Δh_1 and Δh_2 are related by[4]

$$\gamma = \frac{\Delta h_1}{\Delta h_2} = \frac{1+R_1/R}{R_1/R_2-R_1/r} \tag{10}$$

For a given rolling process, γ is also an instantaneous variable changing monotonously with time，so its average value over T can be used for mathematical convenience, namely

$$\bar{\gamma} = \int_0^T \frac{1+R_1/R}{R_1/R_2-R_1/(R-h)}\mathrm{d}t/T \tag{11}$$

$$R = \frac{(2R_0-h_0)h_0}{2h}+\frac{h}{2} \tag{12}$$

$\bar{\gamma}$ describes the distribution state of average feed amount per revolution $\Delta\bar{h}$. The greater the $\bar{\gamma}$, the greater the distribution proportion of $\Delta\bar{h}$ at the outside layer of the ring, and the less the distribution proportion of $\Delta\bar{h}$ at the inside layer of the ring. With increasing of the deformation and spread in the outside layer, the deformation and spread in the inside layer decrease.

1.3   Importance of $\bar{G}$ and $\bar{\gamma}$

It is considered that each process corresponds to a set of values of $\bar{G}$ and $\bar{\gamma}$. For different processes, different ring quality attributes to the variations in $\bar{G}$ and $\bar{\gamma}$.

It can be found from Eqs. (7) and (11) that both $\overline{G}$ and $\overline{\gamma}$ are related to R_1/R_2. Therefore, the change in R_1/R_2 will result in the variations in $\overline{G}$ and $\overline{\gamma}$ and, as a result, affect the rolling processes.

2 FE Modeling

In the dynamic explicit code ABAQUS/Explicit, a coupled thermal-mechanical 3D-FE model is developed for simulating hot rolling of LRTs, as shown in Fig.2. In Fig.2, the driver roll rotates around its stationary axis at a constant speed n_1, the freely mounted idle roll advances at a constant feed rate v towards the driver roll, and the guide rolls have a given motion track in the rolling plane so that they always contact the ring with appropriate pressure to maintain the stability of the operation and the roundness of the ring.

The material of the ring in simulation is Ti-6Al-4V commonly used in large ring production. Its constitutive model within the forging temperature range is given by Ref. [6]. The thermal conductivity, specific heat, thermal expansion coefficient and Young's modulus and their temperature dependence are from Ref. [7].

The FE model has features as follows: (1) The elastic-plastic dynamic explicit approach and mass scaling technology are adopted to greatly improve computational efficiency without sacrificing computational accuracy. (2)The rolls and ring are treated as dynamically isothermal rigid bodies with analytical surfaces and a deformable body, respectively. Because the ring is symmetric with respect to the rolling plane, only the upper half is modelled. (3)The coupled thermo-mechanical hexahedron element with eight nodes is selected to discretize the ring, with finer mesh in the inside and outside layers of the ring. Reduction integration as well as hourglass control is applied to save computation time and avoid the zero-energy mode caused by the bending mode of deformation. The adaptive meshing technology is utilized to reduce element distortion and maintain a high-quality mesh throughout the analysis. (4) Contact pairs are defined between the ring and the driver roll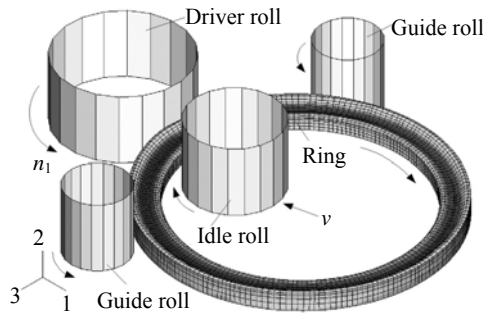, idle roll and guide rolls. There is friction and contact heat conduction at the interface of each contact pair. Relative sliding existing between the ring and rolls contribute to describe the friction with modified Coulomb friction model[8]

$$\tau_f = \begin{cases} \mu p, \tau_f < \tau_s \\ \tau_s, \tau_f \geq \tau_s \end{cases} \qquad (13)$$

where τ_f is the frictional stress, P is the contact pressure, and τ_s is the shear yield stress. At all the surfaces of the ring, convection and radiation are considered, while the symmetry plane is assumed to be adiabatic. (5) The motion of the guide rolls can effectively be realized by a simple method[9].

The FE model has been verified to be reliable by a comparison with experimental results concerning with surface temperature and geometry histories of the ring[9].

3 Results and Discussion

Under the calculation condition shown in Table 1, the effects of R_1/R_2 on the ring quality have been studied and optimized values of R_1/R_2 have been achieved.

3.1 Effects of R_1/R_2 on the ring quality

3.1.1 Relative spread

Fig.3 shows the variations of the average relative spread (*Bar*) and the standard deviation of relative spread (*SDBr*) with R_1/R_2. The smaller the *Bar*, the less the metal flowing to the axial direction of the ring; the smaller the *SDBr*, the more uniform the spread distribution and the better the end-plane quality of the ring. It can be seen that *Bar* and *SDBr* decrease and then increase with increasing of R_1/R_2, which can be clarified from Fig.4.

Fig.2 Coupled thermal-mechanical 3D-FE model for hot rolling of LRTs

Table 1 Calculation condition

| Forming parameter	Value
Ratio of radius of driver roll to radius of idle roll, R_1/R_2	Changing within [1.18, 2.81]
Radius of guide rolls/mm	160
Initial outer radius of ring /mm	397.5
Initial inner radius of ring /mm	210
Rotational speed of driver roll/rad·s^{-1}	4.21
Feed rate of idle roll/mm·s^{-1}	8
Reduction ratio in radial thickness of ring	0.533
Friction coefficient	0.5
Initial temperature of ring/°C	880
Temperature of rolls/°C	250
Temperature of environment/ °C	30
Contact heat conductivity/W·m^{-2}·°C^{-1}	4000 [11]
Convection coefficient/W·m^{-2}·°C^{-1}	20 [7]
Emissivity	0.6 [7]
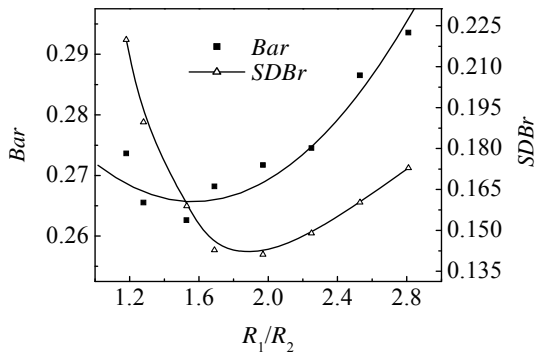
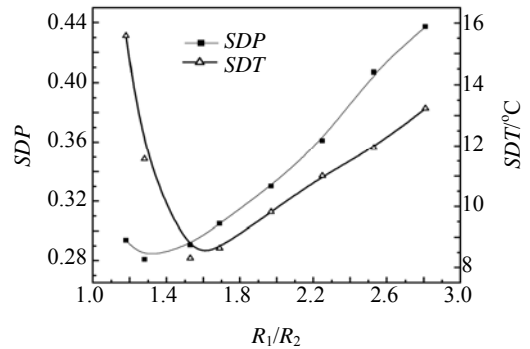Fig.3   Variations of *Bar* and *SDBr* with R_1/R_2

Fig.5   Variations of *SDP* and *SDT* with R_1/R_2

Fig.4 shows the relative spread distributions along the radial thickness of the ring under various R_1/R_2. It is found that when R_1/R_2 is set as a relatively large value, the large spread occurs in the inside layer of the ring (IL) and the small spread occurs in the middle layer (ML) and that with decreasing of R_1/R_2, the IL decreases while the outside layer (OL) and ML increase in spread, which is in agreement with the experimental result reported by Xu et al.[10] and that when R_1/R_2 decreases to a certain value, the large spread transfers from the IL to the OL and the small spread transfers from the ML to the IL. This can be explained from the viewpoint of GSDZ. First, the decrease of R_1/R_2 makes $\overline{G}$ increase by 74.77%, so the OL and IL decrease while the ML increases in spread. Second, the decrease of R_1/R_2 causes $\overline{\gamma}$ to increase by 436.32%, thus leading to the OL increasing while the IL decreasing in spread. The variation in the spread distribution is the balance of the above two aspects, and it is clear that $\overline{\gamma}$ has a stronger effect than $\overline{G}$.

3.1.2   Strain

Fig.5 shows the variation of the standard deviation of equivalent plastic strain (*SDP*) with R_1/R_2. Generally, the smaller the *SDP*, the more uniform the strain distribution, leading to the microstructure becoming more uniform. It is found that *SDP* decreases and then increases with decreasing of R_1/R_2, which can be clarified from Fig. 6.

Fig.6 shows the equivalent plastic strain (*PEEQ*) distributions along the radial thickness of the ring under various R_1/R_2. It is found that when R_1/R_2 is set as a relatively large value, the large deformation occurs in the IL and the small deformation occurs in the ML and that with decreasing of R_1/R_2, the IL decreases while the OL and ML increase in *PEEQ* and that when R_1/R_2 decreases to a certain value, the large deformation transfers from the IL to the OL. Also, this can be explained from the viewpoint of GSDZ.

3.1.3   Temperature

Fig.5 also shows the variation of the standard deviation of temperature (*SDT*) with R_1/R_2. Generally, the smaller the *SDT*, the more uniform the temperature distribution, leading to the microstructure becoming more uniform. It is clear that with decreasing of R_1/R_2, *SDT* decreases and then increases. This can be explained from Fig.7. Fig.7 shows the temperature distributions along the radial thickness of the ring under various R_1/R_2. It is found that the variation of the temperature distribution with R_1/R_2 is similar to that of the strain distribution. In fact, hot rolling of large ring is a plastic forming process with coupled thermo-mechanical effect and most deformation energy is dissipated in the form of heat energy, while titanium alloy has a poor heat conduction property, so there is a similarity between strain and temperature distributions.
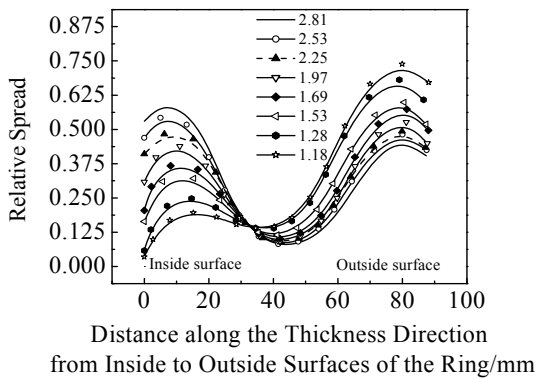

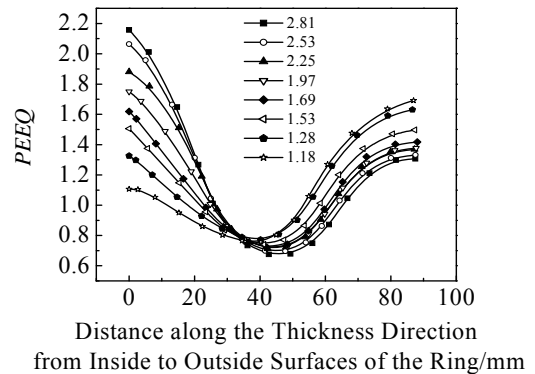Fig.4   Relative spread distributions along radial thickness of ring under various R_1/R_2

Fig.6   *PEEQ* distributions along radial thickness of ring under various R_1/R_2
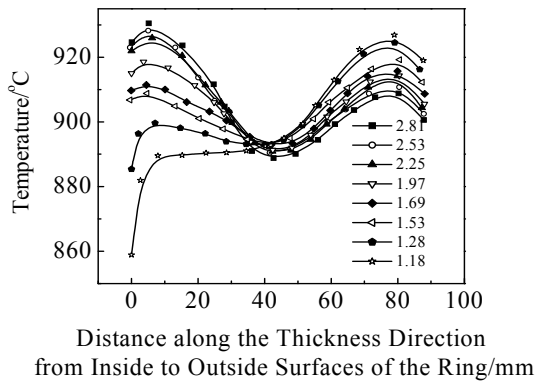
Fig.7   Temperature distributions along radial thickness of ring under various R_1/R_2

3.2   Optimization of R_1/R_2

As can be known from the above analysis, the distributions of relative spread, strain and temperature become uniform and then become nonuniform with decreasing of R_1/R_2. The optimized values of R_1/R_2 can be obtained according to $(Y-Y_{min})/Y_{min} \leqslant 10\%$, where Y is the value of an index, and Y_{min} is the minimum value of the index. The values of R_1/R_2 corresponding to Y which satisfies the above equation consist of the optimized values of R_1/R_2. Therefore, the optimized ranges of R_1/R_2 for *SDB*, *SDP* and *SDT* are 1.5-2.2, 1.2-1.8 and 1.5-1.9, respectively. The intersection of the three ranges is 1.5-1.8, within which the LRTs with better end-plane quality and more uniform strain and temperature distributions can be achieved.

3   Conclusions

1) With the decrease of R_1/R_2, the distributions of relative spread, strain and temperature of LRTs become uniform and then become nonuniform.

2) There is an optimized range of R_1/R_2, i.e., 1.5-1.8, within which the LRTs with better end-plane quality and more uniform strain and temperature distributions can be obtained. The optimized range of R_1/R_2 may be different under different calculation conditions, but the FE simulation method provides an effective means for its determination.

References

1   Xu Siguang(许思广), Wang Haiwen(王海文). *Journal of Taiyuan Heavy Machinery Institute*(太原重型机械学院学报)[J], 1989, 10(1): 1
2   Xie C L, Dong X H, Li S J *et al. Int J Mach Tools Manufact*[J], 2000, 40: 81
3   Wang Z W, Zeng S Q, Yang X H *et al. J Mater Process Tech*[J], 2007, 182(1-3): 374
4   Hua Lin(华 林), Huang Xingao(黄兴高), Zhu Chundong(朱春东). *Theory and Technology of Ring Rolling*(环件轧制理论与技术)[M]. Beijing: Mechanical Industry Press, 2001
5   Hawkyard J B, Johnson W, Kirkland W. *Int J Mech Sci*[J], 1973, (15): 873
6   Hu Z M, Brooks J W, Dean T A. *J Mater Process Tech*[J], 1999, 88: 251
7   Lee R S, Lin H C. *J Mater Process Tech*[J], 1998, 79: 224
8   Gearing B P, Moon H S, Anand L. *Int J Plasticity*[J], 2001, 17: 237
9   Wang M, Yang H, Sun Z C *et al. T Nonferr Metal Soc*[J], 2006, 16(6): 1274
10 Xu Siguang, Wang Hauwen, Shan Zhifu. *Journal of Taiyuan Heavy Machinery Institute*[J], 1989, 10(1): 1
11 Hu Z M, Brooks J W, Dean T A. *Proceedings of the Institution of Mechanical Engineers Part C*[C], 1998, 212(6): 485

大型钛环热辗扩成形轧辊尺寸效应及优化

王　敏，杨　合，郭良刚，孙志超

（西北工业大学，陕西 西安 710072）

摘　要：在大型钛环热辗扩成形过程中，驱动辊半径 R_1 与芯辊半径 R_2 的比值 R_1/R_2 对变形区几何形状有重要影响，而后者对于获得高质量环件起着决定性的作用。本实验首先对变形区几何形状进行了解析描述，定量确定了其与 R_1/R_2 之间的关系；其次，基于动力显式 FE 程序 ABAQUS/Explicit，建立了可靠的大型钛环热辗扩成形过程的热力耦合 3D-FE 模型；最后，采用 FE 模拟方法，从变形区几何形状角度研究了该成形过程中 R_1/R_2 对环件成形质量的影响及机制。研究结果表明，存在 R_1/R_2 的一个优化取值范围。R_1/R_2 在此范围内取值，能够获得端面质量良好、应变和温度分布较均匀的大型钛环。

关键词：大型钛环；热辗扩；轧辊尺寸；动力显式 FEM；热力耦合